

Theory of channeling effect, III. Energy losses of fast particles

Yu. Kagan and Yu. V. Kononets

I. V. Kurchatov Institute of Atomic Energy, Moscow

(Submitted October 22, 1973)

Zh. Eksp. Teor. Fiz. **66**, 1693–1710 (May 1974)

The formalism developed earlier by the present authors is applied to the analysis of energy losses of fast charged particles passing through crystals under channeling conditions. The problem is reduced to the solution of a Fokker–Planck-type equation in the space of the transverse momenta and transferred energy. Analysis of the stopping power and the energy straggling coefficient shows that for deep subbarrier states these parameters are largely determined by scattering by valence electrons. For low-lying states above the barrier, these two quantities turn out to be appreciably greater than the corresponding values in a random medium. It is shown that the form of the energy distribution is, to large extent, determined by the character of diffusion escape of particles from the channel. The solution of the problem obtained for the case of planar channeling reproduces all the details of the energy distributions of particles obtained experimentally so far.

1. INTRODUCTION

In previous papers^[1,2] (subsequently referred to as I and II, respectively), we were concerned with the quantum theory of the channeling effect and considered the evolution of the spatial distribution of fast charged particles penetrating a crystal. It was shown that a plane wave incident on the crystal (when the linear size of the collimated spot was much greater than the interatomic distance) was transformed on the boundary as a result of coherent diffraction into a set of Bloch functions which then propagates over a distance $L < L_{\text{coh}}$ without appreciable loss of coherence due to inelastic scattering. The description of the transverse motion of the particles over lengths of this order was based on the Schrödinger equation and the analysis of the corresponding quantum effects (cf. I).

The quantity L_{coh} which characterizes the attenuation thickness for the nondiagonal elements of the particle density matrix due to inelastic scattering by phonons and electrons was determined in II. For protons with energies of the order of a few MeV, it was found to be of the order of a few thousand Angstroms. The vanishing of the nondiagonal elements of the density matrix leads to a peculiar symmetrization of the state for $L > L_{\text{coh}}$ which precedes the angular spreading of the particles out of the channel (for further details see II). The subsequent evolution of the angular and energy distributions of the particles is then described by an integro-differential equation for the diagonal elements of the density matrix, i.e., for the particle distribution over the different states. The transition probabilities in the collision integral are then determined for the Bloch functions describing the transverse motion of the particles in the course of channeling. The motion of the particles inside and outside the channel is thus naturally taken into account in this integro-differential equation.

The solution of this equation, which describes the angular distribution of particles apart from the dependence on the energy lost by them (distribution integrated over the energy), was considered in II. In this paper, we use the same general equation to determine the energy distribution of the particles as well, and consider the evolution of this distribution with increasing crystal thickness. In contrast to the previous problem, we cannot now transform to the distribution integrated with respect to the angles because of the spatial inhomogeneity of the energy loss, which appears in the presence of channeling. On the other hand, the character of the dif-

ferential angular distribution of the particles plays a determining role in the distribution of the energy losses, which becomes very sensitive to the diffusion of particles out of the channel. This predetermines the necessity of finding the general distribution of the particles, both with energy and with the angles which, in turn, leads to difficulties not encountered in the usual theory of energy losses in random media.

For angles of incidence less than the channeling angle ϑ_0 , the physics of the situation can be described as follows. For $L > L_{\text{coh}}$, the angular distribution splits into two beams after the nondiagonal elements of the density matrix have been damped out. In the first beam, the particles are found in sub-barrier levels inside the channel, whilst in the second beam they occupy states lying above the barrier near the apex of the potential barrier (in the simple classical picture this corresponds to the splitting of the beam into the channelled and random components when they enter the crystal^[3]). Since the wave functions for the sub-barrier states decay exponentially through the potential barrier in the direction of the equilibrium position of the crystal atoms, the energy losses for particles in deep sub-barrier levels are connected largely with the excitation of valence electrons and partly with the so-called distant collisions accompanied by the excitation of electrons in the inner atomic shells. This results in a reduction in the stopping power (as compared with the amorphous medium) by a substantial factor (the corresponding experimental analysis is given by Appleton et al.).^[4]

Multiple scattering in the channel, which is equivalent to slow diffusion in the space of transferred momenta, leads to the population of increasingly higher-lying energy states, and hence to an increasing stopping power, because of the slower decay of the wave functions and the reduction in the thickness of the potential barrier, which is particularly important when the oscillations of the atoms are taken into account. If we recall the sharp peak exhibited by the wave functions for the low-lying sub-barrier states in the region where the atoms are located (see I for further details), we must conclude that, as we leave the channel, the stopping power becomes greater than in the case of the amorphous medium (Kumakhov^[5] has drawn attention to this point). Because of the strong diffusion in the region outside the channel, the particles rapidly leave the sub-barrier region and are slowed down in the usual way, well known for amorphous media. The situation observed for particles which have left the

channel will, of course, also be observed for particles which are found in states above the barrier for $L > L_{\text{coh}}$.

It is shown in II that the dechanneled particles may again be captured into the channel (in principle, within an appreciable angular distance from the center of the incident spot) where, after an appreciable time dictated by slow diffusion in the channel, their energy losses will be small although the resultant losses for such particles will be substantially greater than the losses experienced by particles diffusing in this region without leaving the channel. On the other hand, particles which have rapidly "crossed" the channel as a result of the coherent influence of the medium (see II for further details) exhibit the energy losses characteristic for the region outside the channel. The result of all this is a peculiar energy distribution which is very different in different directions.

The fact that particles moving inside and outside the channel experience different energy losses, so that the channeling effect is very important for the energy distribution, has been well known since the beginning of studies of orientation phenomena (see, for example, [3]). However, the few theoretical analyses made so far have all been based on highly simplified models, using two time-independent unrelated beams. In other words, the most interesting part of the phenomenon, which is connected with the continuous diffusion of particles out of the channel, has, in fact, been ignored. At the same time, the energy losses experienced by an individual beam were described either in terms of a simple model (see, for example, [5,6]) or in terms of a trajectory-type calculation (see, for example, [7]). The only exception is the paper by Altman et al., [8] who attempted to take into account the escape of the particles out of the channel in a simple way, and to analyze the energy distribution in the limiting case of a thick crystal.

In the present paper we report a general analysis of the energy distribution of fast heavy charged particles under channeling conditions, which is largely confined to the planar case. We begin by considering the transition from the integrodifferential equation to the differential equation in the angular and energy variables within the framework of the usual transformation to a Fokker-Planck-type equation (Sec. 2). The variable coefficients of this equation, their explicit dependence on the state of the particle, and the transition to the values for the amorphous medium are analyzed in Secs. 3 and 4. In Sec. 5 we consider the solution of the equation and analyze the properties of the energy distribution. The quantitative results, obtained under certain simplifying assumptions, are found to reproduce practically all the experimental information available so far.

2. EQUATION FOR THE ENERGY DISTRIBUTION FUNCTION

In II, we obtained an equation for the diagonal density matrix $\rho_{1\mathbf{q}\mathbf{q}}(t) \equiv \rho_1(\mathbf{q}, t)$ in the form given by (5.1) for crystals of thickness $L \gg L_{\text{coh}}$. In the present paper, it will be convenient to use the transverse momentum \mathbf{q}_\perp (in the expanded zones scheme) and the total energy E of the particles as the variables. Integrating the right-hand side of this equation with respect to energy in an explicit form, we obtain the basic equation in the form

$$\frac{\partial \rho_1(\mathbf{q}_\perp, E)}{\partial t} = \int d^2 \mathbf{q}'_\perp \sum_{\alpha, \alpha'} w(\alpha, \alpha'; \mathbf{q}_\perp, \mathbf{q}'_\perp)$$

$$\times [\rho_{2\alpha'}^{(0)}(\mathbf{q}'_\perp, E + \Delta E_{\alpha\alpha'}) - \rho_{2\alpha}^{(0)}(\mathbf{q}_\perp, E)]. \quad (2.1)$$

In this equation, $\Delta E_{\alpha\alpha'} = E_\alpha - E_{\alpha'}$ is the change in the energy of the medium, $\rho_{2\alpha}^{(0)}$ is its equilibrium density matrix, and the transition probability is ($\hbar = 1$)

$$w(\alpha, \alpha'; \mathbf{q}_\perp, \mathbf{q}'_\perp) = \frac{M}{(2\pi)^2 q^0} |W(\alpha, \alpha'; \mathbf{q}_\perp, \mathbf{q}'_\perp; q_z, q'_z)|^2, \quad (2.2)$$

where

$$q'_z = [2M(E + \Delta E_{\alpha\alpha'} - \epsilon_{\mathbf{q}'_\perp})]^{1/2}, \quad (2.3)$$

$\epsilon_{\mathbf{q}_\perp}$ is the energy corresponding to the Bloch state with quasimomentum \mathbf{q}_\perp , and q^0 and M are, respectively, the momentum and mass of the particles penetrating the crystal.

The matrix element for the inelastic scattering operator W (defined as the difference between the total interaction operator between the particle and the medium and its average, strictly periodic, value) is determined in terms of the Bloch functions describing the motion of the particle in the transverse x, y plane (see II). We shall suppose that the thickness will be restricted so that we shall be able to neglect the change in E in the matrix elements and in the probabilities. In accordance with (2.2) and (2.3), the transition probability can then be determined exclusively in terms of the variables \mathbf{q}_\perp and α . (This means, of course, that we shall not consider any variation in the nature of the channeling or losses due to the reduction in the particle energy; see, for example, [3].)

For the sake of simplicity, we shall confine our attention to planar channeling. It is shown in II that, when $L > L_{\text{coh}}$, the distribution of particles in the channel is described by a symmetric (even in q_x) distribution function $\rho_+(\mathbf{q}_x, \mathbf{q}_y, t)$. The energy distribution $f(E, t)$, i.e., the distribution integrated with respect to all the escape angles, is determined only by the symmetric part of the distribution both in and out of the channel. In fact,

$$f(E, t) = \int \frac{d^2 \mathbf{q}_\perp}{(2\pi)^2} \rho_+(\mathbf{q}_\perp, E, t) = \int \frac{d^2 \mathbf{q}_\perp}{(2\pi)^2} \rho_+(\mathbf{q}_\perp, E, t). \quad (2.4)$$

We note that the energy distribution of particles for a fixed angle of escape will also depend on the odd part of the distribution function ρ_- if the initial angle of incidence lies outside the channel.

For the symmetric distribution function, we have from (2.1) after some simple transformations, using the invariance of the Schrödinger equation under time reversal,

$$\frac{\partial \rho_+(\mathbf{q}_\perp, E)}{\partial t} = 2 \int d^2 \mathbf{q}'_\perp \int_{-\infty}^{\infty} d^2 \mathbf{q}''_\perp \sum_{\alpha, \alpha'} w_+(\alpha, \alpha'; \mathbf{q}_\perp, \mathbf{q}'_\perp) \times [\rho_{2\alpha'}^{(0)}(\mathbf{q}'_\perp, E + \Delta E_{\alpha\alpha'}) - \rho_{2\alpha}^{(0)}(\mathbf{q}_\perp, E)], \quad (2.5)$$

where $w_+(\alpha, \alpha'; \mathbf{q}_\perp, \mathbf{q}'_\perp)$ is the even part of the probability $w(\alpha, \alpha'; \mathbf{q}_\perp, \mathbf{q}'_\perp)$ in the variable q_x , which turns out to be automatically even in q'_x as well.

A substantial change in the energy loss situation for channeled particles begins at distances of the order of the dechanneling diffusion length L_D . The energy losses over a thickness of the order of L_D in all the most interesting cases are large in comparison with the maximum energy loss in a collision with an electron. We can therefore ignore fluctuations in the loss distribution (see, for example, [9,10]) and consider only the average picture.

Let us expand the function $\rho_+(\mathbf{q}'_\perp, E + \Delta E_{\alpha\alpha'})$ on the right of (2.5) into a series in powers of $\Delta E_{\alpha\alpha'}$ and re-

tain only terms up to the second order, inclusive. We then have

$$\begin{aligned} \frac{\partial \rho_+(q_{\perp}, E)}{\partial t} &= 2 \int_0^{\infty} dq_x' \int_{-\infty}^{\infty} dq_y' w_+(q_{\perp}, q_{\perp}') [\rho_+(q_{\perp}', E) - \rho_+(q_{\perp}, E)] \\ &+ 2 \int_0^{\infty} dq_x' \int_{-\infty}^{\infty} dq_y' \frac{\partial \rho_+(q_{\perp}', E)}{\partial E} \sum_{\alpha, \alpha'} w_+(\alpha, \alpha'; q_{\perp}, q_{\perp}') \Delta E_{\alpha\alpha'} \rho_{2\alpha'}^{(0)} \\ &+ \int_0^{\infty} dq_x' \int_{-\infty}^{\infty} dq_y' \frac{\partial^2 \rho_+(q_{\perp}', E)}{\partial E^2} \sum_{\alpha, \alpha'} w_+(\alpha, \alpha'; q_{\perp}, q_{\perp}') (\Delta E_{\alpha\alpha'})^2 \rho_{2\alpha'}^{(0)}. \end{aligned} \quad (2.6)$$

The probability $w_+(q_{\perp}, q_{\perp}')$ summed over the states of the crystal in this expression is equal to the probability encountered in the multiple scattering problem (see II; as in II, we are neglecting the change in q_z in collisions, which is unimportant for the multiple scattering problem).

We now transform from (2.6) to a Fokker-Planck-type equation in the variables q_{\perp} . In the first term on the right, this transformation is identical with that executed in II. In the last two terms, on the other hand, which are small, we can set $q_{\perp}' = q_{\perp}$ in ρ_+ . (In the second term, we are neglecting $\partial^2 \rho_+ / \partial q_{\perp} \partial E$ for the same reasons that the linear hydrodynamic term was omitted in II; see the corresponding discussion in II.) The result is

$$\frac{\partial \rho_+}{\partial t} = \frac{\partial}{\partial q_x} D_x^+(q_x) \frac{\partial \rho_+}{\partial q_x} + D_y^+(q_x) \frac{\partial^2 \rho_+}{\partial q_y^2} + \mu(q_x) \frac{\partial \rho_+}{\partial E} + \nu(q_x) \frac{\partial^2 \rho_+}{\partial E^2}, \quad (2.7)$$

where

$$\mu(q_x) = \int d^2 q_{\perp}' \sum_{\alpha, \alpha'} w(\alpha, \alpha'; q_{\perp}, q_{\perp}') \Delta E_{\alpha\alpha'} \rho_{2\alpha'}^{(0)} \quad (2.8)$$

is the so-called stopping power (apart from a factor) and

$$\nu(q_x) = \frac{1}{2} \int d^2 q_{\perp}' \sum_{\alpha, \alpha'} w(\alpha, \alpha'; q_{\perp}, q_{\perp}') (\Delta E_{\alpha\alpha'})^2 \rho_{2\alpha'}^{(0)} \quad (2.9)$$

is the energy straggling coefficient. The values and properties of the diffusion coefficients $D_{\beta}^+(q_x)$ ($\beta = x, y$) are analyzed in II.

In the ensuing analysis, it will be convenient to consider the distribution function integrated with respect to q_y , i.e.,

$$\varphi(q_x, E, t) = \int_{-\infty}^{\infty} \rho_+(q_{\perp}, E, t) dq_y, \quad (2.10)$$

where we must recall that all the coefficients in (2.7) depend only on q_x . Integrating both sides of (2.7) with respect to q_y , we obtain

$$\frac{\partial \varphi}{\partial t} = \frac{\partial}{\partial q_x} D_x^+(q_x) \frac{\partial \varphi}{\partial q_x} + \mu(q_x) \frac{\partial \varphi}{\partial E} + \nu(q_x) \frac{\partial^2 \varphi}{\partial E^2}, \quad (2.11)$$

the solution of which, integrated with respect to q_x , will determine the energy distribution of the particles as a function of thickness (time).

3. STOPPING POWER

It is well known^[11] that the energy losses of a fast charged particle are predominantly due to the excitation of the electronic subsystem of the crystal. When we determine the stopping power (and the energy straggling coefficient), we therefore find that the oscillations of the atoms affect only the displacement of the center of gravity of their electron density. Allowance for this fact reduces to the averaging of the resulting expressions over the phonon subsystem (the corresponding average operation will be indicated by the symbol $\langle \dots \rangle_T$).

Thus, the quantity \hat{W} in the expression for μ given by (2.8) is simply the Coulomb interaction between the moving particle and the crystal electrons. We shall evaluate the matrix element for this interaction between the plane waves which describe the motion of the particle along the y and z axes (the x axis is perpendicular to the crystallographic planes forming the channel):

$$\begin{aligned} &\int_{-\infty}^{\infty} dy \int_{-\infty}^{\infty} dz \frac{\exp\{i(\Delta_y y + \Delta_z z)\}}{[(x-x_a)^2 + (y-y_a)^2 + (z-z_a)^2]^{3/2}} \\ &= 2\pi \frac{\exp\{i(\Delta_y y_a + \Delta_z z_a) - |x-x_a|(\Delta_y^2 + \Delta_z^2)^{1/2}\}}{(\Delta_y^2 + \Delta_z^2)^{3/2}}, \end{aligned} \quad (3.1)$$

where \mathbf{r}_a is the electron coordinate and $\Delta_{\beta} = q'_{\beta} - q_{\beta}$ is the change in the momentum component on collision. For heavy particles, we have, using the restriction on the transferred momentum given by (2.3),

$$\Delta_z \approx \Delta E_{\gamma 0} / v^0 \equiv \Delta_v, \quad (3.2)$$

where $\Delta E_{\gamma 0} = E_{\gamma} - E_0$ is the excitation energy of the electronic subsystem and v^0 is the longitudinal velocity of the particle.

Using (3.1) and (3.2), we have, instead of the stopping power given by (2.8),

$$\begin{aligned} \mu(q_x) &= \frac{Me^4}{q^0} \int_{\Gamma} \int dq_x' d\Delta_v \frac{E_{\gamma} - E_0}{\Delta_v^2 + \Delta_{\Gamma}^2} \left\langle \left| \int_0^{\infty} dx d\tau \exp\{i(\Delta_y y_a + \Delta_{\Gamma} z_a) \right. \right. \\ &\quad \left. \left. - |x-x_a|(\Delta_v^2 + \Delta_{\Gamma}^2)^{1/2}\} \psi_{q_x'}(x) \psi_{q_x}(x) \psi_{\Gamma} \psi_0 \right|^2 \right\rangle_{\Gamma}. \end{aligned} \quad (3.3)$$

In this expression $\psi_{q_x}(x)$ are the Bloch wave functions describing the motion of the particle along the x axis (see I for further details), ψ_0 and ψ_{γ} are the wave functions for the ground and excited states of the electronic subsystem, and $d\tau$ is the element of configuration space for the latter.

We can now use the completeness theorem to perform explicit integration with respect to q_x' in (3.3):

$$\begin{aligned} \mu(q_x) &= \frac{2\pi Me^4}{q^0} \int d\Delta_v \sum_{\Gamma} \frac{E_{\gamma} - E_0}{\Delta_v^2 + \Delta_{\Gamma}^2} \int_{-\infty}^{\infty} dx |\psi_{q_x}(x)|^2 \left\langle \left| \left(\sum_0^{\infty} \exp\{i[\Delta_y y_a + \Delta_{\Gamma} z_a] \right. \right. \right. \\ &\quad \left. \left. - |x-x_a|(\Delta_v^2 + \Delta_{\Gamma}^2)^{1/2}\} \right) \right|^2 \right\rangle_{\Gamma}. \end{aligned} \quad (3.4)$$

It is immediately clear that the energy losses are appreciably dependent on the density of the channeled particles $|\psi_{q_x}(x)|^2$ in the electron localization regions. This becomes increasingly better defined as the transferred momentum $(\Delta_y^2 + \Delta_{\Gamma}^2)^{1/2}$ increases. This immediately exhibits the essential difference between the valence electrons and the electrons in the inner atomic shells, and for the latter the difference between the so-called distant and close collisions.

To obtain a still clearer description of the situation, we introduce into (3.4) the usual procedure whereby Δ_{Γ} is replaced by some average value Δ which, in principle, is a function of q_x , so that, using the summation theorem (see, for example, ^[12]), we obtain

$$\sum_{\Gamma} (E_{\gamma} - E_0) |f_{\Gamma 0}|^2 = \sum_{\Gamma} (f_{\Gamma}^+ - f_{\Gamma}^-) f_{\Gamma 0}.$$

After some simple transformations, we have

$$\begin{aligned} \mu(q_x) &= \frac{4\pi Me^4}{mq^0} \int_0^{\Delta_{\max}} d\Delta_v \int_{-\infty}^{\infty} |\psi_{q_x}(x)|^2 \\ &\times \left\langle \left(\sum_0^{\infty} \exp\{-2|x-x_a|(\Delta_v^2 + \Delta^2)^{1/2}\} \right) \right\rangle_{\Gamma} dx. \end{aligned} \quad (3.5)$$

The collision kinematics predetermines the usual restriction on the maximum transferred momentum

$$\Delta_v^{\max} = \xi m v^0, \quad (3.6)$$

where m is the electron mass and ξ is of the order of unity. [If we transform to a random medium, we can show that (3.5) leads to the well-known expression for μ when $\xi = 1$.]

So far, we have not distinguished between different groups of electrons. Moreover, valence electrons in the crystal are most frequently collectivized and have a very different spatial distribution. It is, therefore, useful to separate the contributions of valence and inner electrons to the energy losses, and describe each by an expression such as (3.5) with Δ respectively equal to Δ_V and Δ_i .

For valence electrons, and if we adopt the homogeneous spatial distribution, we immediately obtain, by integrating with respect to the electron variables,

$$\mu_v \approx (4\pi M e^4 N Z_v / m q^0) \ln(2\Delta_v / \Delta_i), \quad (3.7)$$

where N is the number of atoms per unit volume and Z_v is the number of valence electrons per atom (for the sake of simplicity, we are assuming a monatomic crystal). We have also employed the normalization for the wave function $\psi_{q_x}(x)$. We note that the result given by (3.7) is the same as that obtained for a random medium.

We now consider the inner electrons and start with collisions corresponding to momentum transfers $\Delta_v > \Delta'_y \sim 1/a_i$, where a_i is the characteristic size of the ion core (we are using a single size although one could, of course, consider each of the inner shells of the ion separately). The finite contribution to (3.5) is then provided by the region of small values of the difference $x - x_a$, and we have the approximate result

$$\begin{aligned} \mu_i'(q_x) &\approx \frac{4\pi M e^4 N}{m q^0} \int_{\Delta'_y}^{\Delta_v^{\max}} d\Delta_v \left\langle \left(\sum_b |\Psi_{q_x}(x_b)|^2 \right. \right. \\ &\times \int_{-\infty}^{\infty} dx \exp\{-2|x - x_b|[\Delta_v^2 + \Delta_i^2]^{1/2}\} \Big\rangle_T \\ &= \frac{4\pi M e^4 N}{m q^0} \left\langle \left(\sum_b |\Psi_{q_x}(x_b)|^2 \right) \right\rangle_T \ln \frac{\Delta_v^{\max}}{\Delta'_y} \end{aligned} \quad (3.8)$$

where the sum over b represents summation over electrons corresponding to one ion core; we are assuming throughout that $\Delta_v^{\max} \gg \Delta'_y > \Delta_i$.

It is quite clear from this expression that, at any rate for deep sub-barrier states, this part of the energy losses will be suppressed because of the exponential fall in the wave function $\psi_{q_x}(x)$ during motion toward the equilibrium position of the nucleus. We note that, in the case of a random medium, $\psi_{q_x}(x)$ is a plane wave and

$$\left\langle \sum_b |\Psi_{q_x}(x_b)|^2 \right\rangle_T \rightarrow Z - Z_v. \quad (3.9)$$

For smaller momentum transfers, we use the fact that $\Delta_y a_i \ll 1$, $\Delta_i a_i < 1$ and omit x_a from the argument of the exponential in (3.5) (x is measured from the equilibrium position of the excited ion). In that case,

$$\mu_i''(q_x) \approx \frac{4\pi M e^4 N (Z - Z_v)}{m q^0} \int_0^{\Delta'_y} d\Delta_v \int_{-\infty}^{\infty} |\Psi_{q_x}(x)|^2 \exp\{-2|x|(\Delta_v^2 + \Delta_i^2)^{1/2}\} dx. \quad (3.10)$$

This expression enables us to investigate quite readily the various limiting cases. Suppose that for deep sub-barrier states $\Delta x_0(q_x) > 1$ [$x_0(q_x)$ is the coordinate of the nearest classical turning point during motion in a well in state q_x]. It then immediately follows from (3.10) that, for the so-called distant collisions, the contribution to the energy losses due to excitation of inner electron shells is exponentially small. As a result, the losses in

this case are practically determined by the valence electrons. In the opposite limiting case, i.e., when $\Delta_i x_0(q_x) \ll 1$, we have from (3.10) the fact that, in the region of small transferred momenta, i.e., $\Delta_y x_0(q_x) \ll 1$, the result is very similar to that for a random medium. This is most readily shown by replacing $|\psi_{q_x}(x)|^2$ in (3.10) with its x average, and integrating in explicit form.

It is important that $\Delta_i = \overline{\Delta E}_{\gamma 0} / v^0$ is inversely proportional to the velocity of the incident particle. It follows that, as the particle energy increases, the effect of channeling on the reduction in energy losses due to distant collisions with inner electrons becomes smaller.

In a random medium, $|\psi_{q_x}(x)|^2 = 1$ and (3.10) together with (3.8) and (3.9) lead to the well-known classical result for the stopping power due to the inner-shell electrons.

The above results enable us to investigate the entire evolution of energy losses during channeling. First, we note the following result, which is physically relatively obvious: losses due to valence electrons are practically the same as in a random medium, independently of the state in which the particle is found. As regards the losses due to the inner electrons, these are very sensitive to the state of the particle in the effective potential in the channel. For the lowest lying sub-barrier states, losses due to close collisions are completely suppressed, whilst those due to distant collisions are reduced to a considerable extent. As a result, the stopping power is reduced by a factor of δ as compared with a random medium, where $Z/Z_v > \delta \gtrsim 2$. If we now consider the high-lying sub-barrier states, we find that the first losses to reappear are those connected with distant collisions. Close collisions are significant only for states near the apex of the barrier.

There is particular interest in the states above the barrier but near the apex. As noted in I, for these states we have the characteristic rapid increase in the particle density near the atom localization regions. This ensures that energy losses in these states due to the inner electron shells will be greater than in the random medium. This is clearly seen from (3.8) and (3.10). Further increase in $|q_x|$ ensures that the motion of the particles is nearly free and we finally arrive at the same results as for the random medium, which were discussed above.

4. ENERGY STRAGGLING COEFFICIENT

Since in (2.9) the transferred energy is raised to the second power, the energy straggling coefficient ν is, in practice, determined only by close collisions. This enables us to understand immediately the fact that, during motion inside the channel, this coefficient is determined practically exclusively by scattering by valence electrons.

From the formal point of view, the predominance of close collisions enables us to neglect the excitation energy of the electron subsystem in the expression for ν in comparison with $v^0 \Delta_y$, recalling at the same time that, in the case of scattering of heavy particles by electrons, there is a stringent restriction on the magnitude of the transferred momentum (or transferred energy). Using this fact, we rewrite (2.9) in the form

$$\nu(q_x) = \frac{M e^4}{2q^0} \left\langle \int \frac{d^2 q_{\perp}}{\Delta_v^2} \sum_y (E_y - E_0)^2 |f(q_x, q_x', \Delta_y)|^2 \right\rangle_T, \quad (4.1)$$

where

$$f(q_x, q_x', \Delta_v) = \sum_{\alpha} \int_{-\infty}^{\infty} \psi_{q_x'}^*(x) \psi_{q_x}(x) \exp(i\Delta_v y - |\Delta_v||x-x_a|) dx. \quad (4.2)$$

The evaluation of the sum over γ can be carried out in a general form using the summation theorem

$$\sum_{\gamma} (E_{\gamma} - E_0)^2 |f_{\gamma 0}|^2 = 1/2 (f f^{*} + f^{*} f)_{00}.$$

Omitting terms which yield zero on integration with respect to q_x' , and commuting (4.2) with the electron Hamiltonian, we obtain

$$\frac{1}{2} (f f^{*} + f^{*} f) = \frac{\Delta_v^2}{m^2} \sum_{\alpha} \left\{ |\psi_{q_x'}^*(x_a) \psi_{q_x}(x_a)|^2 - \frac{\partial}{\partial x_a} |g_1(q_x, q_x', \Delta_v; x_a)|^2 \frac{\partial}{\partial x_a} - |g_2(q_x, q_x', \Delta_v; x_a)|^2 \frac{\partial^2}{\partial y_a^2} \right\};$$

$$g_1(q_x, q_x', \Delta_v; x_a) = \int_{-\infty}^{\infty} \psi_{q_x'}^*(x) \psi_{q_x}(x) \exp(-|\Delta_v||x-x_a|) \text{sign}(x-x_a) dx, \quad (4.3)$$

$$g_2(q_x, q_x', \Delta_v; x_a) = \int_{-\infty}^{\infty} \psi_{q_x'}^*(x) \psi_{q_x}(x) \exp(-|\Delta_v||x-x_a|) dx.$$

We now recall that

$$\int_{-\infty}^{\infty} |g_1|^2 dq_x' = \int_{-\infty}^{\infty} |g_2|^2 dq_x' = 2\pi \int_{-\infty}^{\infty} |\psi_{q_x}(x)|^2 \exp(-2|\Delta_v||x-x_a|) dx = g_{q_x}(\Delta_v; x_a).$$

In that case, substituting (4.3) in (4.1), we obtain

$$\nu(q_x) = \frac{e^4}{2m^2 v^0} \left\langle \int d^2 q_{\perp} \sum_{\alpha} (|\psi_{q_x'}^*(x_a) \psi_{q_x}(x_a)|^2)_{00} - 2\pi \int d\Delta_v \sum_{\alpha} \left(\frac{\partial}{\partial x_a} g_{q_x}(\Delta_v; x_a) \frac{\partial}{\partial x_a} + g_{q_x}(\Delta_v; x_a) \frac{\partial^2}{\partial y_a^2} \right)_{00} \right\rangle_T. \quad (4.4)$$

Using the approximate result

$$g_{q_x}(\Delta_v; x_a) \approx 2\pi |\psi_{q_x}(x_a)|^2 / |\Delta_v|$$

and the behavior of the wave function $\psi_{q_x}(x)$, we may conclude that for particle states inside the channel the contribution due to the inner-electron shells to (4.4) is, in fact, quite small. For valence electrons, we can readily show that the contribution of the second term in this formula is small in comparison with the contribution of the first in the ratio of $(v_e/v^0)^2$, where v_e is the characteristic velocity of the valence electrons. There is an analogous result for the inner electrons during the motion of the particle outside the channel. Therefore, the energy straggling coefficient can finally be written in the form

$$\nu(q_x) = \frac{e^4}{2m^2 v^0} \sum_{\alpha} \int d^2 q_{\perp} \langle (|\psi_{q_x'}^*(x_a) \psi_{q_x}(x_a)|^2)_{00} \rangle_T. \quad (4.5)$$

In a random medium, replacing $\psi_{q_x}(x)$ by a plane wave, and remembering that in this integral the maximum transferred momentum is $2mv^0$, we have

$$\nu_1 \approx 2\pi N Z e^4 v^0, \quad (4.6)$$

which is identical with the well-known expression for this quantity.

Inside the channel, the energy straggling coefficient for fast particles is close to

$$\nu_0 = (Z_0/Z) \nu_1, \quad (4.7)$$

although it is possible that it may be somewhat greater due to the particular features of the matrix element in (4.5). For states above the barrier, which lie near the apex, the function $\nu(q_x)$ will be greater than ν_1 for the same reasons as in the case of the stopping power (see preceding section) and further increase of $|q_x|$ leads to the same results as for a random medium.

5. ANALYSIS OF ENERGY LOSSES IN THE CASE OF PLANAR CHANNELING

We begin with the qualitative analysis of the effect of channeling on energy losses of fast particles, using certain simplifying assumptions. Firstly, we neglect the energy straggling coefficient $\nu(q_x)$ in (2.11). It is clear from the foregoing discussion that the broadening of the energy distribution due to the last term in (2.11) is not well defined inside the channel. Outside the channel, this broadening is connected, above all, with the diffusion picture of particle escape from the channel (see below), and the finite value of ν affects the situation only qualitatively. Next, we assume that the stopping power $\mu(q_x)$ can be approximated by a power function equal to μ_0 inside the channel whilst outside the channel $\mu_1 > \mu_0$. Even from the result given in II we may conclude that this power-function approximation for the kinetic characteristics in the case of planar channeling is fully adequate and enables us to describe practically all the details of the phenomenon. We shall also use the fact that, according to the analysis given in II, the diffusion coefficient D_1 in the space of transverse momenta outside the channel, is greater by one or two orders of magnitude than the diffusion coefficient D_0 inside the channel. Therefore, in the simple qualitative analysis of the energy loss, we may ignore recapture of dechanneled particles into the channel.

Let $Q(\tau)$ be the flux of particles passing through the channel boundary at time τ . The energy distribution of dechanneled particles at time t is then given by

$$\int_0^t d\tau Q(\tau) \delta(\epsilon - \mu_0 \tau - \mu_1(t-\tau)) = \frac{1}{\mu_1 - \mu_0} Q \left(\frac{\mu_1 t - \epsilon}{\mu_1 - \mu_0} \right) [\theta(\epsilon - \mu_0 t) - \theta(\epsilon - \mu_1 t)], \quad (5.1)$$

where $\epsilon = E^0 - E$ is the energy lost, and $\theta(x)$ is the step function such that $\theta = 1$ for $x \geq 0$ and $\theta = 0$ for $x < 0$. The overall energy distribution is obtained by adding the part of the distribution connected with particles remaining in the channel to (5.1):

$$f(\epsilon, t) = \left[1 - \int_0^t Q(\tau) d\tau \right] \delta(\epsilon - \mu_0 t) + \frac{1}{\mu_1 - \mu_0} Q \left(\frac{\mu_1 t - \epsilon}{\mu_1 - \mu_0} \right) [\theta(\epsilon - \mu_0 t) - \theta(\epsilon - \mu_1 t)]. \quad (5.2)$$

It is clear from (5.2) that the energy loss distribution is wholly determined by the diffusion of particles out of the channel. The last problem was solved in II, and this enables us to write down the expression for the flux Q . Recalling that the fraction $f_2(q_x, q_y, t)$ [see (6.3) in II] gives a zero net contribution to Q , we find, after some simple calculations,

$$Q(\tau) = -2D_0 \int_{-\infty}^{\infty} dq_y \frac{\partial \rho_+}{\partial q_x} \Big|_{q_x = -q_x^*} = \frac{2(D_0/D_1)^{1/2}}{\pi \tau_0} \int_0^{\infty} d\xi \frac{\xi \exp(-\xi^2 \tau / \tau_0) \cos(\xi q_x^0 / q_x^*) \sin \xi}{\cos^2 \xi + (D_0/D_1) \sin^2 \xi}.$$

In this expression, q_x^0 determines the position of the initial δ -function distribution (the initial angle of incidence relative to the set of crystallographic axes which we are considering is $\theta = q_x^0 / q^0 < \theta_0 = q_x^* / q^0$ where q_x^* is the momentum corresponding to the channeling angle θ_0) and

$$\tau_0 = (q_x^*)^2 / D_0. \quad (5.3)$$

The above expression is readily transformed to the form

$$Q(\tau) = \frac{1}{2\pi i \tau_0} \int_{c-i\infty}^{c+i\infty} ds \frac{\exp(s\tau/\tau_0) \operatorname{ch}(\sqrt{s} q_x^0 / q_x^*)}{\operatorname{ch}\sqrt{s} + (D_0/D_1)^{1/2} \operatorname{sh}\sqrt{s}}$$

(Re $C > 0$, $-\pi/2 < \arg \sqrt{s} \leq \pi/2$),

and hence, using the condition $D_0/S_1 \ll 1$ in an explicit form, we obtain

$$Q(\tau) = \frac{\pi}{\tau_0} \sum_{n=0}^{\infty} (-1)^n (2n+1) \cos \frac{(2n+1)\pi q_x^0}{2q_x^*} \exp \left\{ -\frac{(2n+1)^2 \pi^2 \tau}{4\tau_0} \right\}. \quad (5.4)$$

When $\tau \rightarrow 0$ or ∞ the function $Q(\tau)$ tends to zero together with all its derivatives. However, the most important fact is that Q has a well defined peak at $\tau = \tau_m$, the position, height, and width of which depend on the initial angle of incidence, i.e., on q_x^0 . As the angle of incidence approaches the channeling angle (i.e., as $|q_x^0|$ approaches q_x^*), this peak becomes narrower and appears at smaller values of τ . All this is clear by inspection of Fig. 1, which shows a plot of $Q(\tau)$ for four values of the initial angle of incidence.

This behavior of the function Q leads to a very peculiar time evolution of the energy distribution. The factor Q in the second term in (5.2) has a peak which moves along the energy scale in accordance with the formula

$$\varepsilon_m = \mu_1 t - (\mu_1 - \mu_0) \tau_m (q_x^0). \quad (5.5)$$

However, for small times (or thicknesses) $t < \tau_m$ this peak is absent from the distribution since it does not fall into the allowed energy interval and the distribution given by (5.2) has only the internal channel peak. In accordance with (5.5), the peak in the distribution of particles outside the channel moves with constant velocity μ_1 and enters the real energy region at time $t = \tau_m (q_x^0)$ and subsequently departs from the internal channel peak with relative velocity $\mu_1 - \mu_0$. When $t \gg \tau_m (q_x^0)$, its position tends to approach $\mu_1 t$ which is characteristic for particles moving outside the channel right from the start. The constant shift $(\mu_1 - \mu_0) \tau_m$ tends to be masked if we recall the spreading of the energy distribution due to the last term in (2.11).

The expression for Q given by (5.4) enables us to estimate τ_m . For the sake of simplicity, let us take the simplest case $q_x^0 = 0$. By retaining the first two terms in the sum given by (5.4), we then have

$$\frac{\tau_m(0)}{\tau_0} = \frac{3 \ln 3}{2\pi^2} \approx 0.167. \quad (5.6)$$

It is readily verified that the contribution of all terms in the series beginning with the third is, in fact, negligible for this value of τ .

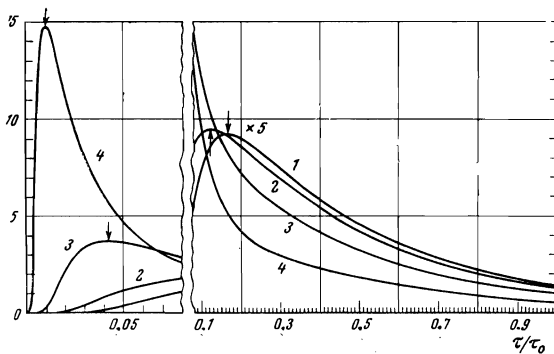


FIG. 1. Q in units of τ_0^{-1} as a function of τ for different initial values of q_x^0 : (1) $q_x^0 = 0$, (2) $q_x^0 = 0.25 q_x^*$, (3) $q_x^0 = 0.5 q_x^*$, (4) $q_x^0 = 0.75 q_x^*$. Arrows indicate the position of the peaks on the curves.

The simple structure of the series for $\tau > \tau_m$ enables us to see immediately that the energy distribution of particles outside the channel falls exponentially from a maximum toward lower energy losses, in accordance with the expression

$$\exp\{-\pi^2(\varepsilon_m - \varepsilon) / [4\tau_0(\mu_1 - \mu_0)]\}. \quad (5.7)$$

As t increases, an increasing number of particles leaves the channel, leading to a continuous fall in the height of the internal channel peak which, for sufficiently large $t > \tau_0$, occurs in accordance with the exponential law

$$1 - \int_0^t Q(\tau) d\tau \approx \frac{4}{\pi} \cos \frac{\pi q_x^0}{2q_x^*} \exp\left\{-\frac{\pi^2 t}{4\tau_0}\right\}. \quad (5.8)$$

At the same time, however, the shape of the external channel peak and, in particular, its height, which are dictated by the form of the function $Q(\tau)$, remain unaltered. [This result is modified only when the finite energy straggling coefficient $\nu(q_x)$ is taken into account].

We have so far ignored the fact that, for any angle of incidence $\theta < \theta_0$, states above the barrier are populated as well as those under the barrier (see I). Since we are neglecting diffusion capture of particles above the barrier into the channel, these particles lose energy in accordance with the stopping power μ_1 right from the beginning. This predetermines the appearance of an additional "normal" peak in the energy distribution, which, under our assumptions, is characterized by the δ function $\delta(\varepsilon - \mu_1 t)$. However, in practice, the presence of spreading due to the finite energy straggling coefficient ν may ensure that the "normal" peak and the external channel peak described above will not be resolved. (We note that, in the simple approximation which we are considering, the particles divide into three groups, depending on the character of the losses during channeling, as noted previously by Altman et al.^[8]).

The above picture reproduces most of the leading characteristic features of the energy distribution of fast particles under channeling conditions. Quantitative analysis will, however, have to take into account the particle energy spread, i.e., the solution of the complete equation (2.11), and the presence of the anomalous increase in losses for states above the barrier and near its apex. The latter can be taken into account by introducing a further interval $q_x^* < |q_x| < \tilde{q}_x$ with its own values of the coefficients \tilde{D} , $\tilde{\mu}$, $\tilde{\nu}$, each of which is, in principle, greater than the corresponding value for $|q_x| > \tilde{q}_x$ which corresponds to a random medium (as before, we retain the subscript 1 for these quantities, while those corresponding to the channel will be indicated by the subscript 0). In the intermediate region, the most important quantity is $\tilde{\mu}$, or more precisely $\tilde{\mu} \tilde{t}$, where

$$\tilde{t} = (\tilde{q}_x - q_x^*)^2 / \tilde{D} \quad (5.9)$$

is the characteristic time for finding the particle in the intermediate region, since only by taking into account the fact that $\tilde{\mu} > \mu_1$ can we explain the existence of the anomalously high energy losses. The difference between \tilde{D} , $\tilde{\nu}$ and D_1 , ν_1 cannot, in itself, play an important role for dechanneled particles which have entered the region $|q_x| > \tilde{q}_x$ because the time spent by the particles in the intermediate region is negligible in comparison with the characteristic dechanneling time τ_0 given by (5.3), which is the dominant factor in the energy loss problem.

We have considered the solution of (2.11) by assuming

constant values for the coefficients for each of the three regions noted above. It was therefore found to be convenient to apply the Fourier transformation with respect to the variable $\epsilon = E^0 - E$ and the Laplace transformation with respect to the variable t , and then solve the resulting differential equation in q_x in explicit form, followed by the matching of the distribution functions and fluxes at $|q_x| = q_x^*$ and $|q_x| = \tilde{q}_x$. Inverting the transformations, and integrating with respect to q_x [see (2.4)], we then find the expression for the energy loss distribution function. Since (2.4) contains only ρ_+ , the initial condition for φ was taken in the form

$$\varphi(q_x, \epsilon, 0) = \frac{1}{2} [\delta(q_x - q_x^0) + \delta(q_x + q_x^0)] j(\epsilon). \quad (5.10)$$

In its final form, the energy distribution function can be written as follows:

$$f(\epsilon, t) = \frac{1}{(2\pi)^2 i} \int_{-\infty}^{\infty} dp \exp(-p^2 H t - i p(\epsilon - t)) \int_{C-i\infty}^{C+i\infty} e^{i\chi} \chi(p, \zeta) d\zeta, \quad (5.11)$$

where the function $\chi(p, \zeta)$ depends on the region in which the initial value q_x^0 is found:

$$\chi(p, \zeta) = \alpha_j^{-2}(p, \zeta) + \Lambda_j(p, \zeta) / \lambda(p, \zeta), \quad (5.12)$$

$$j = \begin{cases} 0 & \text{if } |q_x^0| < 1, \\ 1 & \text{if } \tilde{q}_x > |q_x^0| \geq 1, \\ 2 & \text{if } |q_x^0| \geq \tilde{q}_x. \end{cases}$$

In these expressions (for the sake of simplicity we are omitting the arguments of α_j)

$$\begin{aligned} \alpha_0 &= \zeta^{\frac{1}{2}}, & \alpha_1 &= [\zeta + p^2 H (\bar{v}/v_0 - 1) - i p (\bar{\mu}/\mu_0 - 1)]^{\frac{1}{2}}, \\ \alpha_2 &= [\zeta + p^2 H (v_1/v_0 - 1) - i p (\mu_1/\mu_0 - 1)]^{\frac{1}{2}}, & -\pi/2 < \arg \alpha_j \leq \pi/2; \\ \lambda(p, \zeta) &= \alpha_1^2 (\xi \alpha_2 \operatorname{ch} \alpha_0 + \xi \alpha_0 \operatorname{sh} \alpha_2) \operatorname{ch} [\xi \alpha_1 (\tilde{q}_x - 1)] \\ &+ \alpha_1 (\alpha_1^2 \operatorname{ch} \alpha_0 + \xi \xi \alpha_0 \alpha_2 \operatorname{sh} \alpha_2) \operatorname{sh} [\xi \alpha_1 (\tilde{q}_x - 1)]; \\ \Lambda_0(p, \zeta) &= \{ \xi (\alpha_1^2 - \alpha_2^2) \alpha_2^{-1} - (\alpha_1^2 - \alpha_0^2) \alpha_0^{-2} [\xi \alpha_2 \operatorname{ch} [\xi \alpha_1 (\tilde{q}_x - 1)] \\ &+ \alpha_1 \operatorname{sh} [\xi \alpha_1 (\tilde{q}_x - 1)]] \} \operatorname{ch} (\alpha_0 q_x^0), \\ \Lambda_1(p, \zeta) &= \xi (\alpha_1^2 - \alpha_0^2) \alpha_0^{-1} \operatorname{sh} \alpha_0 [\operatorname{ch} [\xi \alpha_1 (\tilde{q}_x - |q_x^0|)] \\ &+ \xi \alpha_2 \alpha_1^{-1} \operatorname{sh} [\xi \alpha_1 (\tilde{q}_x - |q_x^0|)]] \\ &+ \xi (\alpha_1^2 - \alpha_2^2) \alpha_2^{-1} [\operatorname{ch} \alpha_0 \operatorname{ch} [\xi \alpha_1 (|q_x^0| - 1)] \\ &+ \xi \alpha_0 \alpha_1^{-1} \operatorname{sh} \alpha_0 \operatorname{sh} [\xi \alpha_1 (|q_x^0| - 1)]], \\ \Lambda_2(p, \zeta) &= \{ (\alpha_2^2 - \alpha_1^2) \alpha_2^{-2} [\xi \alpha_0 \operatorname{sh} \alpha_2 \operatorname{ch} [\xi \alpha_1 (\tilde{q}_x - 1)] \\ &+ \alpha_1 \operatorname{ch} \alpha_0 \operatorname{sh} [\xi \alpha_1 (\tilde{q}_x - 1)]] \\ &+ \xi (\alpha_1^2 - \alpha_0^2) \alpha_0^{-1} \operatorname{sh} \alpha_0 \} \exp \{ -\alpha_2 (|q_x^0| - \tilde{q}_x) (D_0/D_1)^{\frac{1}{2}} \}; \\ \xi &= (D_1/D)^{\frac{1}{2}}, & \bar{\xi} &= (D_1/D)^{\frac{1}{2}}, & H &= v_0 / (\tau_0 \mu_0^2). \end{aligned} \quad (5.13)$$

In (5.11)–(5.13), the parameter t is expressed in units of τ_0 given by (5.3), ϵ is given in units of $\mu_0 \tau_0$, q_x^0 and \tilde{q}_x are given in units of q_x^* , and the distribution function $f(\epsilon, t)$ itself is given in units of $(\mu_0 \tau_0)^{-1}$.

As usual, the contour of integration with respect to ζ in (5.11) must lie to the right of all the singular points of the integrand. It can be shown that, with the chosen form of the integral representation, this is satisfied, at any rate, for $\operatorname{Re} C > 0$.

The foregoing discussion of the role of the transition region enables us to assume that $\tilde{v} = v_1$ and $\tilde{D} = D_1$ in specific calculations. The inaccuracy in $\tilde{\zeta}$ given by (5.9) can then be compensated by the corresponding redefinition of the width of the intermediate region $\tilde{q}_x - q_x^*$. Consequently, the intermediate region can be adequately characterized by only two parameters, namely, $\tilde{\mu}$ and $\tilde{q}_x - q_x^*$.

Figure 2 shows the energy distribution curves for zero angle of incidence ($\theta = 0$) and successive values of the dimensionless time t between 0.25 and 3. To exhibit most clearly the time evolution of the distribution, we give separately the curves for particles under the barrier ($q_x^0 = 0$, curve 1) and those above the barrier (q_x^0

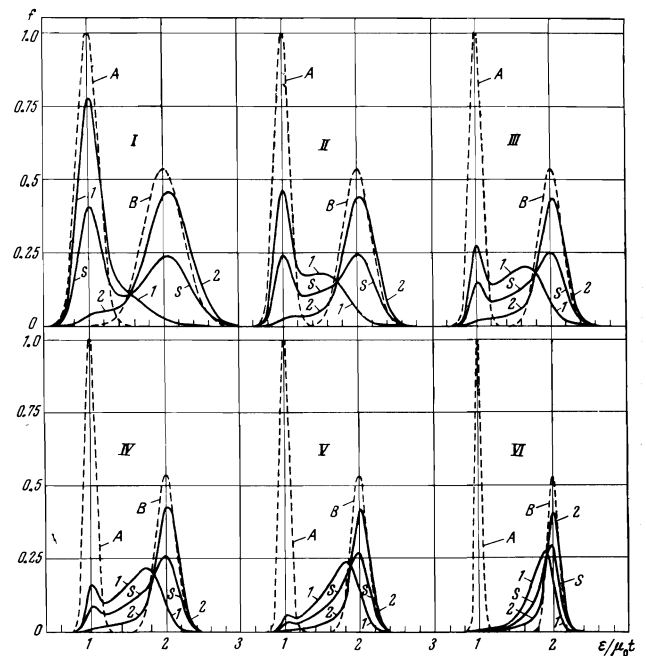


FIG. 2. Energy loss distribution for fast particles in the case of planar channeling calculated from (5.11)–(5.14) for different times t (crystal thickness) and fixed initial angle of incidence $\vartheta = 0$, (I) $t = 0.25 \tau_0$, (II) $t = 0.5 \tau_0$, (III) $t = 0.75 \tau_0$, (IV) $t = \tau_0$, (V) $t = 1.5 \tau_0$, (VI) $t = 3 \tau_0$. Curve 1 corresponds to particles above the barrier ($q_x^0 = 0$) and curve 2 to particles above the barrier. S indicates resultant curves obtained on the assumption that the initial population of states above the barrier amounts to 50%. The points represent the distributions in random media with parameters characteristic for purely interval channel motion (curve a) and for motion outside the channel with $|q_x| > \tilde{q}_x$ (curve B). The distributions corresponding to each individual time are plotted in their own relative units and are normalized to equal area.

= 1, curve 2), normalized to equal area, and the resultant curves S based on the assumption that the population of the states above the barrier is 50%. This choice was dictated by the fact that we were concerned with the channeling of protons with energies of a few MeV in silicon along the $\{110\}$ and $\{111\}$ planes. The other parameters were chosen accordingly (see II and the preceding section):

$$\begin{aligned} D_1/D_0 = \tilde{D}/D_0 = 50, & \quad \mu_1/\mu_0 = 2, & \quad \bar{\mu}/\mu_0 = 2.5; \\ v_1/v_0 = \bar{v}/v_0 = 14/4; & & \\ (\tilde{q}_x - q_x^*)/q_x^* = 1, & \quad H = v_0 / (\tau_0 \mu_0^2) = 2.5 \cdot 10^{-2}. \end{aligned} \quad (5.14)$$

For comparison, Fig. 2 shows the distributions corresponding to the motion of particles in random media with parameters characteristic of purely internal channel motion (curve A) and for motion outside the channel in the region $|q_x| > \tilde{q}_x$ (curve B).

If we consider the evolution of the energy distribution for particles inside the channel (curve 1), we readily note that the picture is very close to that obtained above in the simplified analysis. This refers, above all, to the character of the second peak which describes the losses of particles which have left the channel. However, the fact that the ratio D_1/D_0 is finite, and the energy straggling coefficient is not zero, leads to an appreciable decrease in the time for the appearance of this peak, as compared with (5.6). In the resultant picture, on the other hand, for this high initial concentration of particles above the barrier, the second peak cannot be seen in isolated form. Moreover, the emergence of the diffusion front of dechanneled particles ensures that the position

of the peak in the region of high losses eventually shifts to the left, and then again approaches the loss value characteristic for particles in the amorphous medium. We also note that the position of the internal channel peak shifts in comparison with the peak on curve A in the direction of higher energy losses.

For large times (on the scale of the time of particle diffusion out of the channel), the energy distribution increasingly resembles the distribution in the amorphous medium. However, there are two clear differences. The first is connected with the presence of the tail on the distribution in the region of low energy losses, due wholly to the tail of diffusion escape from the channel and the capture of particles into the channel from states above the barrier. The second difference is connected with the region of anomalously high losses. This region is not so readily seen visually because of the importance of the energy broadening which is determined by a function of ν .

The considerable sensitivity of the energy distribution to the initial angle of incidence θ is clearly seen in Fig. 3, which shows the curves for $\theta/\theta_0 = 0.25, 0.5, 0.75, 1, 1.5,$ and 3 (θ_0 is the channeling angle) at the same instant of time (for the same thickness) $t = 0.25\tau_0$. When $\theta < \theta_0$, the initial component above the barrier (curve 2) is assumed fixed for $q_x^0 = [(q_x^*)^2 + (q_x^0)^2]^{1/2}$ where the initial value $q_x^0 = q_x^* \theta / \theta_0$ corresponds to sub-barrier particles (curve 1). When $\theta \geq \theta_0$ the two components of the distribution are practically indistinguishable and, therefore, for these values of θ we give only the resultant curves. All the other parameters are the same as in Fig. 2. The accelerated dechanneling of particles ensures that, as θ increases, the position of the external channel peak on the distribution increasingly approaches the value corresponding to the amorphous medium. At the same time, the height of this peak increases relative to the internal channel peak.

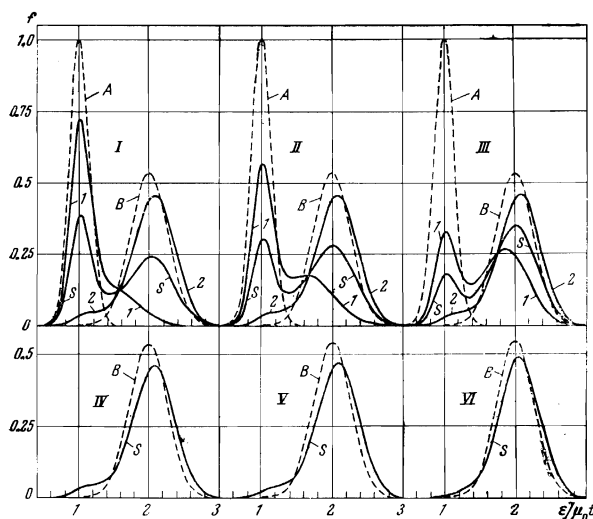


FIG. 3. Energy distributions of the same type as in Fig. 2, calculated for different values of the initial angle of incidence θ for fixed time (crystal thickness) $t = 0.25\tau_0$: (I) $\theta = 0.25\theta_0$, (II) $\theta = 0.5\theta_0$, (III) $\theta = 0.75\theta_0$, (IV) $\theta = \theta_0$, (V) $\theta = 1.5\theta_0$, (VI) $\theta = 3\theta_0$. When $\theta < \theta_0$, the initial component corresponding to particles above the barrier (curve 2) was assumed fixed for $q_x^0 = [(q_x^*)^2 + (q_x^0)^2]^{1/2}$ where the initial value $q_x^0 = \theta/\theta_0$ corresponds to sub-barrier particles (curve 1). When $\theta \geq \theta_0$ the unavoidable appearance of the two components in the distribution is practically unresolved and, therefore, for these values of θ we give only the resultant curves S. The remaining parameters, notation, and normalization of the curves is the same as in Fig. 2.

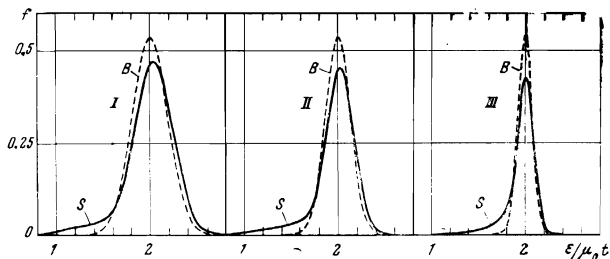


FIG. 4. Energy distributions for different times t corresponding to the angle of incidence $\theta = 3\theta_0$: (I) $t = 0.5\tau_0$, (II) $t = \tau_0$, (III) $t = 3\tau_0$. The notation, normalization, and remaining parameters are the same as in Figs. 2 and 3.

When the angle of incidence is greater than θ_0 , the channeling effect appears largely as the diffusion capture of particles into the channel, and this leads to the appearance of the characteristic low-energy tail in the energy loss distribution curve. It is important that, although diffusion outside the channel occurs very rapidly, the temporal evolution of this tail is determined by the characteristic time for particle diffusion in the channel. The corresponding situation is well illustrated by Fig. 4, which shows the distribution curves for different times corresponding to $\theta = 3\theta_0$ (the remaining parameters are the same as in Figs. 2–3).

If we compare the above distribution curves with the experimental data (see, for example, [4, 13]), we can readily establish that the theory reproduces practically all the details of the experimental picture. Moreover, comparison with the results obtained for silicon shows that the agreement is, in fact, quantitative. (It was not our aim to achieve complete quantitative agreement with experiment and, therefore, the parameters in (5.14) are in only approximate correspondence with the parameters for silicon; moreover, the division of the particles into two groups for $\theta < \theta_0$ is also an approximate device).

In conclusion, we note the possibility of an experimental separation of the energy distribution corresponding to particles which are in the channel at the initial time. This requires two series of measurements for initial angles of incidence $\theta \approx 0$ and $\theta \gtrsim \theta_0$. Comparison of the tails with high energy losses in the two cases should enable us to estimate the relative number of particles in states above the barrier for $\theta \approx 0$. If we then subtract from this first distribution the second distribution multiplied by the weight factor, we obtain a result which is very close to the required distribution. This procedure should enable us to exhibit the detailed feature of the energy distribution of initially channeled particles as a function of thickness (time).

¹ Yu. Kagan and Yu. V. Kononets, Zh. Eksp. Teor. Fiz. **58**, 226 (1970) [Sov. Phys.-JETP **31**, 124 (1970)].

² Yu. Kagan and Yu. V. Kononets, Zh. Eksp. Teor. Fiz. **64**, 1042 (1973) [Sov. Phys.-JETP **37**, 530 (1973)].

³ J. Lindhard, K. Dan. Vidensk. Selsk. Mat.-Fys. Medd. **34**, No. 14 (1965).

⁴ B. R. Appleton, C. Erginsoy, and W. M. Gibson, Phys. Rev. **161**, 330 (1967).

⁵ M. A. Kumakhov, Trudy III Vsesoyuznogo soveshchaniya po fizike vzaimodeystviya zaryazhennykh chastits s monokristallami (Proceedings of the Third All-Union Conference on the Physics of Interaction Between Charged Particles and Single Crystals), Moscow State University, 1972, p. 41.

- ⁶ N. P. Kalashnikov, V. S. Remizovich, and M. I. Ryazanov, *ZhETF Pis'ma Red.* **13**, 715 (1971) [*JETP Lett.* **13**, 508 (1971)].
- ⁷ M. Kitagava and Y. H. Ohtsuki, *Phys. Rev.* **B5**, 3418 (1972).
- ⁸ M. R. Altman, L. C. Feldman, and W. M. Gibson, *Phys. Rev. Lett.* **24**, 464 (1970).
- ⁹ L. Landau, *J. Phys.* **8**, 201 (1944).
- ¹⁰ A. Crispin and G. N. Fowler, *Rev. Mod. Phys.* **42**, 290 (1970).
- ¹¹ N. Bohr, *K. Dan. Vidensk. Selsk. Mat.-Fys. Medd.* **18**, No. 8 (1948).
- ¹² L. D. Landau and E. M. Lifshitz, *Kvantovaya mekhanika (Quantum Mechanics)*, Fizmatgiz, 1963 [Addison-Wesley, 1965].
- ¹³ G. Della Mea, A. V. Drigo, S. L. Russo, P. Mazzoldi, and G. G. Bentini, *Radiat. Eff.* **13**, 115 (1972).

Translated by S. Chomet
175